Evolution of ground-state quadrupole and octupole stiffnesses in even-even barium isotopes

Hua-Lei Wang* and Jie Yang
School of Physics and Engineering, Zhengzhou University, Zhengzhou 450001, China

Min-Liang Liu
Institute of Modern Physics, Chinese Academy of Sciences, Lanzhou 730000, China

Fu-Rong Xu
School of Physics, Peking University, Beijing 100871, China;
Institute of Theoretical Physics, Chinese Academy of Sciences, Beijing 100080, China;
and Center of Theoretical Nuclear Physics, National Laboratory of Heavy Ion Collisions, Lanzhou 730000, China
(Received 6 April 2015; revised manuscript received 13 June 2015; published 3 August 2015)

Quadrupole and octupole stiffnesses in the ground states of even-even $^{112-150}$Ba isotopes have been systematically investigated by means of potential-energy-surface calculations. The calculations are carried out in both (β_2,γ,β_4) and $(\beta_2, \beta_3, \beta_4, \beta_5)$ deformation spaces with the inclusion of triaxial and reflection-asymmetric shape degrees of freedom, respectively. The present results are compared with previous calculations and available experiments. The shape instabilities are evaluated by analyzing the potential energy curves with respect to both the quadrupole and octupole deformations, which is consistent with the previous discussions predicting the γ softness or triaxiality and octupole instability. In addition, taking the near-drip-line ^{114}Ba nucleus as an example, we briefly investigate the effects of potential parameters (e.g., the strength of the spin-orbit potential λ, and the nuclear surface diffuseness a) on the deformation energy curve, showing almost negligible modifications of nuclear shape and stiffness but considerable changes in the depth of the minimum and the height of the fission barrier (which may be very important for the study of heavy and superheavy nuclei).

DOI: 10.1103/PhysRevC.92.024303 PACS number(s): 21.10.Re, 21.60.Cs, 21.60.Ev, 27.60.+j

I. INTRODUCTION

The scalar form of the many-body Hamiltonian does not necessarily imply that all nuclei are spherically symmetric. The spontaneous symmetry breaking mechanism implies that the nuclear mean-field approximation which, formulated in an intrinsic reference frame, allows one to represent nuclei as deformed bodies [1]. In the intrinsic system, some observables such as angular momentum and parity associated with the basic space-time symmetries certainly may not be conserved any more, which means the wave function of a nuclear many-body system is not an eigenstate of such mechanical quantity operators. The measurements of certain multipole moments such as magnetic dipole and electric quadrupole ones [2] are compatible with calculations based on such theoretical concepts, which validates the idea of the usefulness of such a theory. Indeed, the question of whether different intrinsic shape asymmetry may occur in the nuclear ground and/or excited states has been raised [1,3] as one of the most fundamental issues since the well-known concept of spontaneous intrinsic symmetry breaking in atomic nuclei was introduced in the 1950s. During the past several decades considerable effort has been made to reveal such a mechanism and to obtain conclusive evidence for the existence and evolution of different nuclear intrinsic shapes [1,4–7].

The nuclear shape, which plays an important role in determining nuclear properties, can generally be described by the parametrization of the nuclear surface or the nucleon density distribution. In mean-field calculations the multipole expansion of a nuclear surface with spherical harmonics $Y_{\lambda\mu}(\theta,\phi)$ is usually used [8,9]. Because the range of the individual "bumps" on the nuclear surface decreases with increasing deformation multipolarity and should obviously not be smaller than a nucleon diameter, there is a fundamental limitation in λ, and a crude estimate gives the limiting value of $\lambda < A^{1/3}$ [10]. The shape degrees of freedom with lower-order multipolarity λ are therefore expected to be important, as the axial-quadrupole deformation β_2 and the nonaxial-quadrupole (triaxial) deformation γ, the reflection-asymmetric octupole deformation β_3, the hexadecapole deformation β_4, etc.

An abundance of observed phenomena connected with such nuclear deformations are indeed found in nuclei [11,12]. For instance, it is well known that the majority of nuclear shapes can be described by axially symmetric (prolate or oblate) spheroids [13–15], which is confirmed by the observation of rotational band structures and measurements of their properties (e.g., quadrupole moments). The triaxial γ deformation manifests itself by the wobbling motion and chiral doublets, and it may also play an important role in signature splitting (or inversion) [16–20]. The octupole β_3 correlation is usually associated with the experimental observations of alternate-parity bands with enhanced $E1$ transitions, parity doublet bands, and collective $E3$ transitions [21]. Furthermore, there has been considerable research on the question of the nonaxially symmetric octupole deformations in the past [22–27]. For instance, an ensemble of isomeric states of tetrahedral symmetry related to Y_{32} shape components is suggested

*wanghualei@zzu.edu.cn

to exist in the region of light radium nuclei [22]. Dudek *et al.* systematically discussed tetrahedral (even octahedral) symmetry and its possible experimental evidence (e.g., the the corresponding $E1$ transitions should be absent due to no static dipole moments) throughout the periodic table [26,27]. Recently, reflection asymmetric shell model calculations [28] also revealed that the observed low-lying 2^- bands in $N = 150$ isotones [29] may be caused by β_{32} deformation. The covariant density functional theories [30] showed strong Y_{32} correlations in such isotones. A comprehensive overview of various quantum mechanisms associated with hypothetical tetrahedral symmetry, which have been studied within the last ten years or so, can be found in Ref. [31]. The hexadecapole deformations including the nonaxial components have been confirmed by the hexadecapole moment measurements from α scattering studies, but its situation is not so clear, particularly in the problem of the so-called hexadecapole anomaly at the border of the rare-earth region [7]. The higher-order multipole deformations (e.g., β_6) can play a rather important role in the description of excited states and heavy (or superheavy) nuclei [32]. So far, there is almost no conclusive experimental evidence on high-multipolarity deformations with $\lambda > 6$. Of course, theoretical calculations with multipole components up to $\lambda = 16$ (or even more) have already been carried out [33].

The nucleon-nucleon two-body interactions known to be nonlocal and noncentral combine through the Hartree-Fock formalism into the mean-field concept (and Hamiltonian), the latter conveniently allowing one to discuss nuclear stability in terms of single-particle energies and single-particle gaps as functions of nuclear deformations, thus geometrical symmetries. In transition regions, the situations are particularly more complicated than those of spherical or well-deformed nuclear regions. These transitional nuclei are difficult to describe both in models of the macroscopic-microscopic type and in self-consistent models based on two-body interactions such as Hartree-Fock models. The Ba isotopes just locate in such mass regions.

This paper is motivated by the following facts. First and foremost, progress in the development of radioactive nuclear beam facilities has provided us with marvelous findings in nuclear structure, such as neutron halos and neutron skins [34–36]. Much new information on the shapes and structures of nuclei far from stability is being revealed. One of the great interests is to know where and why exotic phenomena of nuclear structure appear and how these phenomena change along the isotopic and isotonic chains. For instance, the quest for lower-order multipole triaxial γ and octupole β_3 deformations and the nature and evolution of collective effects in nuclei is still a long-standing nuclear structural theme. Besides, the Ba isotopes have 56 protons, an octupole "magic number" (the favorable particle number for the occurrence of octupole deformation), and 38 isotopic members from $N = 58$ to 95 (across the $N = 82$ closed shell) have so far been discovered [37]; these include 7 stable, 18 proton-rich, and 13 neutron-rich isotopes. Note that the neutrons and protons have reinforcing effects that favor γ and octupole deformations for the nuclides that have the neutron and/or proton Fermi surfaces just below (above) closed shells [21], i.e., approximately around $N = 76$ and $N = 88$ (below and above the $N = 82$ shell closure, respectively). Moreover, some basic experimental quantities, which do not depend on nuclear models, have to date been measured and studied, such as ground-state binding energies, half-lives, and low-lying excited states (including octupole and quasi-γ bands as well as ground-state bands). These provide a good opportunity to systematically investigate the evolution of ground-state quadrupole (including nonaxial quadrupole γ) and octupole shape degrees of freedom in the barium isotopic chain. Last but not least, it is found that various theoretical approaches have been applied in the description of the ground-state nuclear properties [38–40]. For instance, Möller *et al.* [39,40] have calculated the global systematics of ground-state deformations using the folded Yukawa (FY) single-particle potential and the finite-range droplet model (FRDM). Based on microscopic Skyrme-type forces, Aboussir *et al.* [41] have given the deformation parameters of nuclei with the range $36 \leqslant A \leqslant 300$ in the framework of the extended Thomas-Fermi plus Strutinsky integral (ETFSI) method.

However, in transitional regions the nuclear wave function may be a superposition of states corresponding to different shapes and the potential-energy surface is normally very flat over a large deformation domain. In such a case, the nuclei will undergo permanently large amplitude oscillations and the actual effective deformations have less and less in common with that of the minimum. Moreover, the so-called equilibrium shape identified as the deepest local pocket in such a flat surface will be also strongly affected by the parameter uncertainties of the nucleonic pairing and the deformed mean field. Thus the actual static shape is practically meaningless—the flatter the surface the more meaningless the value of the so-called equilibrium deformations, while the shape stiffness related to the flatness of the energy landscape, which is relatively model independent, may to some extent describe nuclear properties better. We have previously investigated the stiffness evolution of some nuclei in both ground states and rotational states [42–44]. Part of the aim of this work is to test the parameter reliability of the single-particle potential (e.g., the surface diffuseness) and the predictive power of the model in nuclei very far from β stability.

In this paper, we perform the potential-energy-surface (PES) calculations for even-even $^{112-150}$Ba in two different deformation spaces (including triaxial and reflection-asymmetric shape degrees of freedom, respectively), especially focusing on the evolution of quadrupole and octupole stiffnesses. Such a systematic study of nuclear stiffness is so far scarce yet somewhat necessary due to the large uncertainty in equilibrium shape for transitional soft nuclei. It is also useful to establish the systematic law of the stiffness evolution of the Ba isotopes. The paper is organized as follows. A brief introduction of the PES method is presented in Sec. II. The results and discussions are given in Sec. III. Finally, we summarize our work in Sec. IV.

II. MODEL

The PES method based on a macroscopic-microscopic model has been widely used to give the right deformation and energy of a many-body nucleus state [45] in various mass regions, including the drip-line and superheavy ones [32,46,47]. In this method, the total potential energy

$E_{\rm total}(Z,N,\hat{\beta})$ of a nucleus with deformation $\hat{\beta}$ is the sum of a macroscopic bulk-energy term $E_{\rm mac}(Z,N,\hat{\beta})$, being a smooth function of Z,N and deformation, and a microscopic term $\delta E_{\rm mic}(Z,N,\hat{\beta})$ representing the quantum correction based on some phenomenological single-particle potential [45,48].

The macroscopic energy is obtained from the standard liquid-drop model (LDM) with the parameters used by Myers and Swiatecki [49]. Note that such a sharp-surface LDM does not consider the surface diffuseness and the finite range of the nuclear interaction which may play some role in the shape evolution of soft nuclei. The microscopic correction part, which arises because of the nonuniform distribution of single-particle levels, is calculated by means of the well-known Strutinsky method [50–53] whose development has ever been considered as a major leap forward in the nuclear many-body problem. It should be also noted that Strutinsky-type calculations can optimize the liquid-drop energy and give relatively high accuracy which is usually superior to that of the microscopic models employing effective nucleon-nucleon interactions [54]. Though it is seen, in recent years, that the rapid progress of effective forces and self-consistent methods, which occurred thanks to advances in computational technology, allows calculations with similar accuracy, the phenomenological potential is still used widely due to the validity and simplicity during the calculations.

Here, single-particle energies and single-particle wave functions are calculated by solving the Schrödinger equation of the stationary states for an average nuclear potential of Woods-Saxon (WS) type including a central field, a spin-orbit interaction, and the Coulomb potential for the protons. The deformed WS potential is generated numerically at each (β_2,γ,β_4) or $(\beta_2,\ \beta_3,\ \beta_4,\ \beta_5)$ deformation lattice. There exist various parametrizations of the WS potential, e.g., the Blomqvist [55], Chepurnov [56], Rost [57] and universal [58] parameter sets. In our Woods-Saxon calculations we use the universal parameters. The matrix of the one-body Hamiltonian is built by means of the axially deformed harmonic oscillator basis in the cylindrical coordinate system, and then diagonalized.

The pairing correlation is treated using the Lipkin-Nogami (LN) approach [50,52] in which the particle number is conserved approximately and thus the spurious pairing phase transition encountered in the usual BCS calculation can be avoided. The monopole pairing strength G is determined by the average gap method [59,60]. The LN equations are solved in a sufficiently large space of Woods-Saxon single-particle states. In the present work, the pairing windows include $Z/2$ (or 40, if $Z/2 > 40$) and $N/2$ (or 40, if $N/2 > 40$) single-particle levels just above and below the Fermi surface for proton and neutron, respectively. The LN pairing energy can be given by [39,45]

$$E_{\rm LN} = \sum_k 2{v_k}^2 e_k - \frac{\Delta^2}{G} - G\sum_k {v_k}^4 + G\frac{N}{2} - 4\lambda_2 \sum_k {u_k}^2 {v_k}^2, \quad (1)$$

where ${v_k}^2, e_k, \Delta$, and λ_2 represent the occupation probabilities, single-particle energies, pairing gap, and number-fluctuation constant, respectively. The shell correction energy is then calculated by $\delta E_{\rm shell} = E_{\rm LN} - \tilde{E}_{\rm Strut}$, where $\tilde{E}_{\rm Strut}$ is obtained by the Strutinsky method [51,53] with a smoothing range $\gamma = 1.20\hbar\omega_0$ ($\hbar\omega_0 = 41/A^{1/3}$ MeV), and a correction polynomial of order $p = 6$. One may expect the method to be less accurate near the drip lines than close to β stability because the truncated single-particle levels deviate more from a realistic single-particle spectrum near the drip lines than near β-stable nuclei. However, it is found that there is no obvious increase in the model error for nuclei that are the farthest from β stability [39].

Then, the PES is obtained by interpolating between the lattice points in the multidimensional deformation space. The ground-state equilibrium deformation of a nucleus is related to the absolute minimum of the PES. In some circumstances, the secondary minima of the PES may coexist with the global one and even they may be yrast at high-spin states. In the present calculations, the equilibrium shape obtained through the minimization of the total energy over the shape variables is different from the spontaneous symmetry breaking mechanism but they show equivalent results [54].

III. RESULTS AND DISCUSSION

Systematic PES calculations in both (β_2,γ,β_4) and $(\beta_2,\ \beta_3,\ \beta_4,\ \beta_5)$ deformation spaces have been performed for even-even $^{112-150}$Ba which have at least been identified experimentally. For the actual calculations in the former spaces, the Cartesian quadrupole coordinates $X = \beta_2\cos(\gamma + 30^\circ)$ and $Y = \beta_2\sin(\gamma + 30^\circ)$ were used, where the parameter β_2 specifies the magnitude of the quadrupole deformation, while γ specifies the asymmetry of the shape. Also note that in the later deformation spaces the deformation parameters $\beta_2,\beta_3,\beta_4,\beta_5$ are treated as variational parameters, which differs from earlier calculations where only the quadrupole β_2 and octupole β_3 deformations were treated as independent shape parameters and β_4,β_5 were obtained by an approximation [61]. As known, all the theoretical results need to be confronted with experiments or other accepted theories. Experimentally, the viable estimates of the nuclear shapes come from the nuclear moments, e.g., the quadrupole deformation parameter β_2 can be deduced from the intrinsic quadrupole moment related to the reduced electric quadrupole transition probability $B(E2)$ [62]. Sometimes, the empirical Grodzins rule is used to crudely estimate the ellipsoid shapes of nuclei from the first 2^+-state levels [63]. Theoretical estimates usually come from equilibrium deformation predictions given by Strutinsky-type calculations with the modified oscillator (Nilsson) potential, the Woods-Saxon potential, etc., or by microscopic self-consistent mean-field calculations, such as the Skyrme Hartree-Fock and Gogny Hartree-Fock calculations.

Figure 1 shows the isotopic dependence of ground-state deformation parameters β_2, γ, and β_3 obtained from the calculated PES minima for even-even $^{112-150}$Ba, together with the FY+FRDM calculations [39,40] and experimental estimates [62–64] for comparison. The predicted ground-state β_2 deformations in two different deformation spaces mentioned above are very similar, basically in agreement with the experimentally measured results. The comparison presented in the figure shows that our calculation is close to the experimental values though there is still a systematic

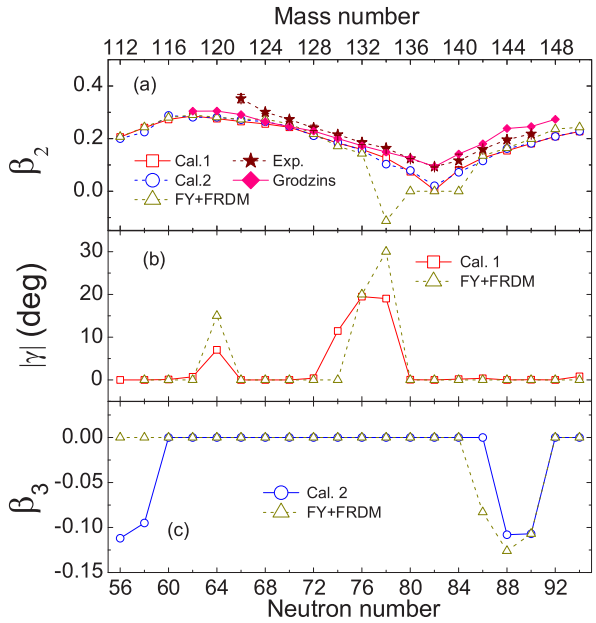

FIG. 1. (Color online) Calculated ground-state β_2 (a), γ (b), and β_3 (c) deformations for even-even $^{112-150}$Ba nuclei, compared with the FY+FRDM calculations [39], the Grodzins estimate [63,64], and the partial experimental values [62]. Cal.1 and Cal.2 denote the calculations are performed in (β_2,γ,β_4) and $(\beta_2,\ \beta_3,\ \beta_4,\ \beta_5)$ deformation spaces, respectively.

underestimation for β_2. Indeed, taking into account the zero-point motion would imply that the experiment-comparable deformations are not the static ones displayed in the figure, but rather the most likely deformations calculated from the solutions of the collective motion. The latter are systematically bigger than the static ones, cf. Ref. [33]. Furthermore, it can be seen that the β_2 value is smallest for ^{138}Ba with $N = 82$ corresponding to the neutron shell closure and the β_2 values of these nuclei, as expected, increase as the neutron number N moves away from the closed shell. Nevertheless, such deformation shows a maximum at ^{118}Ba$_{62}$, with four neutrons less than $N = 66$ ^{122}Ba situated at the neutron midshell, halfway between the $N = 50$ and $N = 82$ major shell closures. It should be pointed out that the β_2 value given by Möller *et al.* [39] is negative in ^{134}Ba, indicating an oblate shape, which is different from the experimental results and the results of our calculations obtained using the Woods-Saxon mean-field Hamiltonian with the universal parameterization. To some extent, the correctness of this result brings a lot of confidence to our calculations.

As shown in Fig. 1(a), the experimental errors are so small that one can define as simply the root-mean-square (rms) deviation to evaluate the model error, which as usual is given by

$$\mathrm{rms} = \left[\frac{1}{n}\sum_{k=1}^{n}\left(\beta_i^{\mathrm{expt}} - \beta_i^{\mathrm{theor}}\right)^2\right]^{1/2}, \qquad (2)$$

where β_i^{theor} is the calculated quadrupole β deformation, and β_i^{expt} is the corresponding measured quantity. There are n such measurements for different N and Z. However, for large experimental errors the above definition is unsatisfactory due to their contributions to the rms deviation. The calculated model errors of β_2 are 0.048 and 0.047 for these even-even Ba isotopes in (β_2,γ,β_4) and $(\beta_2,\ \beta_3,\ \beta_4,\ \beta_5)$ deformation spaces, respectively. In the FY+FRDM calculations, the corresponding rms deviation with the value of 0.099 is somewhat large. However, except for several values with large errors in the $N = 78$, 80, and 84 nuclei, as seen in Fig. 1, the rms deviation can reach 0.047, which agrees well with our calculations. To present a more consistent comparison between theory and experiment, Dudek *et al.* [65] have analyzed the shape inconsistency and deduced relationships between the calculated potential parameters and the nucleonic distributions (labelled by ρ), e.g., for protons in the WS case,

$$\beta_2^{\rho} \simeq 1.10\beta_2 - 0.03(\beta_2)^3. \qquad (3)$$

If the present results are modified by using such a formula, the rms deviation will decrease to 0.036 and 0.034 for these Ba isotopes calculated in (β_2,γ,β_4) and $(\beta_2,\ \beta_3,\ \beta_4,\ \beta_5)$ deformation spaces, respectively. In addition, the calculated γ values are qualitatively in agreement with the calculations by Möller *et al.* [40] except for that in ^{130}Ba, as seen in Fig. 1(b). For the β_3 deformations [see Fig. 1(c)], our calculations show a somewhat large difference from the FY+FRDM calculations [39] in ^{112,114,142}Ba nuclei. So far, the values of γ and β_3 are difficult to directly obtain in experiments. However, the occurrence of strong γ (octupole) correlations has been confirmed in nuclei with particle numbers around 64 and 76 (56, 88, and 134) [21], which is indeed in good agreement with our calculations.

As known, theoretical equilibrium deformations are usually model dependent since they are strongly affected by the mean-field and pairing potential parameters, especially for very soft nuclei. However, the deformation energy curves along different deformation degrees of freedom may relatively describe the nuclear-shape properties better. To display the shape evolutions in β_2, γ, and β_3 directions, we show such deformation energy curves in Figs. 2 and 3. As mentioned above, the Cartesian quadrupole coordinates $X = \beta_2\cos(\gamma + 30^\circ)$ and $Y = \beta_2\sin(\gamma + 30^\circ)$ were used to vary the quadrupole deformation in the actual calculations with the inclusion of γ degrees of freedom. Thus the β_2 value is always positive and the triaxiality parameter covers the range $-120^\circ \leqslant \gamma \leqslant 60^\circ$, as shown in Fig. 2. Certainly, the three sectors $[-120^\circ, -60^\circ]$, $[-60^\circ, 0^\circ]$, and $[0^\circ, 60^\circ]$ represent the same triaxial shapes but represent rotation about the long, medium, and short axes, respectively (Cranking calculation is beyond the scope of this work). Compared with the axial quadrupole deformation minima, the minima of the axial-asymmetric and reflection-asymmetric deformation energy curves are relatively shallower (<0.5 MeV) at the ground states (especially, for the triaxial minima), though they might change with increasing spins [42,44]. Theoretical and systematic studies indicate that the $N = 76$ nuclei are more γ rigid than their neighbors with other neutron numbers [66,67]. Indeed, it seems that the ^{132}Ba$_{76}$ nucleus has the deepest triaxial minimum. Similarly, the expected properties of strongly octupole correlations, as shown in Fig. 3, are reproduced in nuclei with proton numbers near 56 and neutron numbers near 56 or 88 [3,68,69]. The

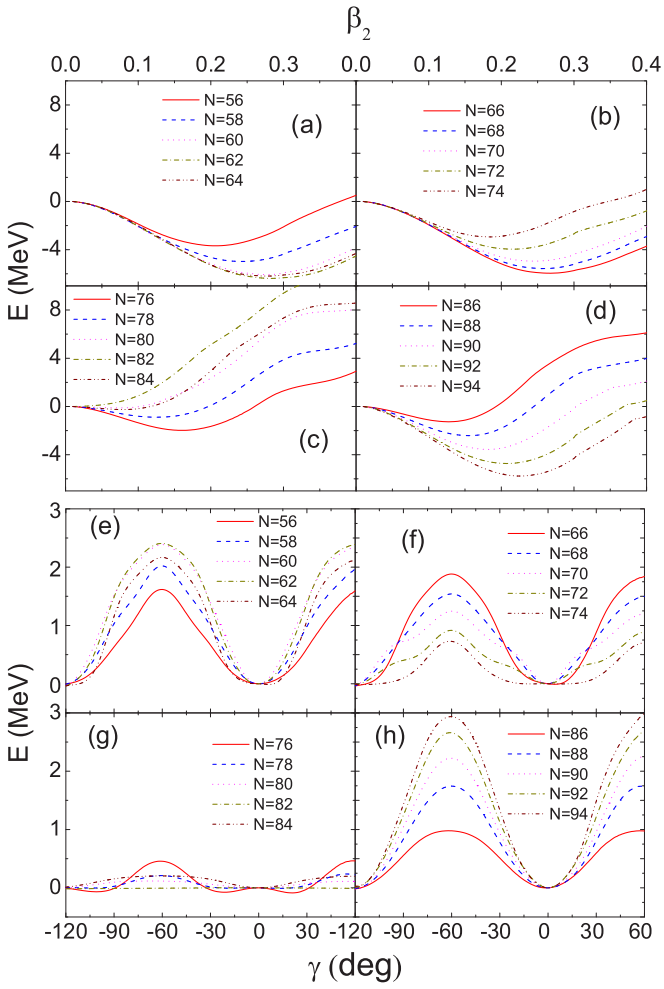

FIG. 2. (Color online) Deformation energy curves against β_2 (the upper panel) and γ (the lower panel) for even-even $^{112-150}$Ba nuclei, calculated in (β_2,γ,β_4) deformation space. At each β_2 (γ) point, the energy has been minimized with respect to the γ (β_2) and β_4 deformations.

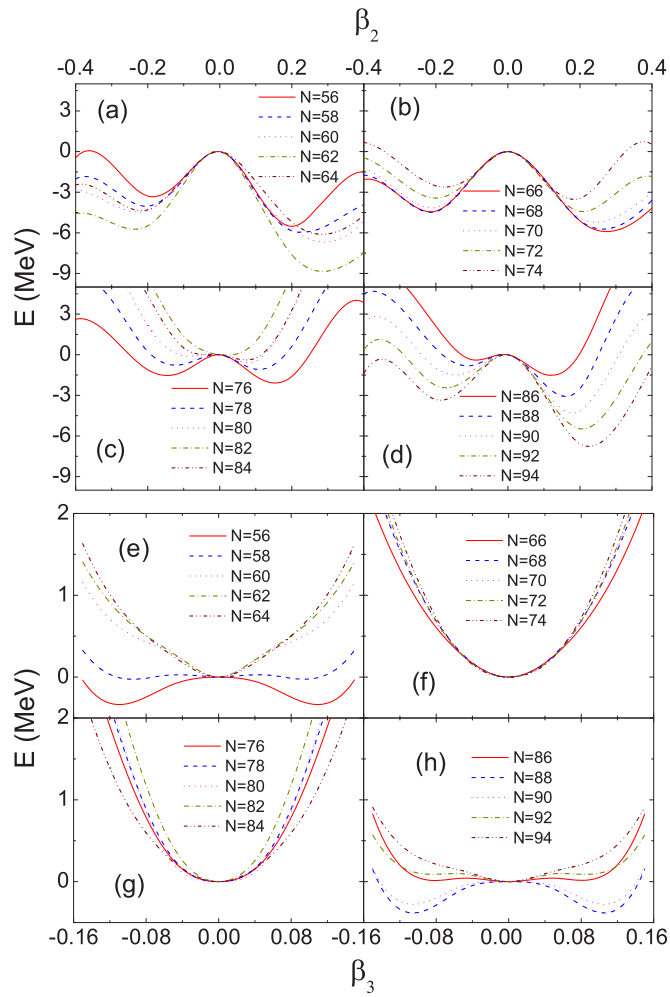

FIG. 3. (Color online) Similar to Fig. 2 but against β_2 (the upper panel) and β_3 (the lower panel) deformations, calculated in (β_2, β_3, β_4, β_5) deformation space.

presence of octupole correlation has been experimentally confirmed in $^{140-146}$Ba [70–74] (around $Z = 56$, $N = 88$) and awaits conclusively experimental evidences around $^{112}_{56}$Ba$_{56}$.

The direct measurement of some quantities (e.g., the triaxial parameter γ) is difficult; even, one cannot determine the quadrupole deformation β_2 from the experimental $B(E2)$ value when the axial symmetry breaks, though the sum-rule method provides an approximation to deduce the value of the triaxial parameter from experimental electromagnetic transition matrix elements [76,77]. Some phenomenological or empirical laws are, therefore, important and used to evaluate the nuclear properties. For instance, the ratio of the excitation energy of first and second excited states, $E_{4_1^+}/E_{2_1^+}$, provides a test of the axial assumption. As pointed out in Ref. [78], this ratio (and other similar ratios) is characteristic of different collective motions of the nucleus, e.g., an axially symmetric rotor should have $E_{4_1^+}/E_{2_1^+} = 3.33$, an harmonic vibrator has $E_{4_1^+}/E_{2_1^+} = 2.00$, while X(5) behavior should have $E_{4_1^+}/E_{2_1^+} = 2.91$.

In Ba isotopes, for which spectroscopic information now extends down to ^{118}Ba and up to ^{148}Ba, the neutron-number dependence of the excited 2_1^+, 2_2^+, 4_1^+, and 3_1^- states known is shown in Fig. 4(a), together with several phenomenological ratios Figs. 4(b)–4(d), as discussed below. The energies of these low-lying levels, which can reveal different collective properties, decrease with the neutron number far away from the $N = 82$ closed shell. From a simple perspective on nuclear structure, we can consider that nuclei in the middle of the spherical shell closures have maximum collectivity where interactions between valence nucleons are maximized, and thus, the excitation energies of the first 2+ states may have local minima [see Fig. 4(a)], indicating large deformations. There is a very general empirical relationship between $\hbar^2/2J$ and β_2 ($6\hbar^2/2J \equiv E_{2^+} \approx 1225/A^{7/3}\beta_2^2$ MeV) that essentially all even-even nuclei follow [63,64]. Figure 4(b) shows that the structural signature $R_{4/2} \equiv E_{4_1^+}/E_{2_1^+}$ for Ba isotopes [except for ^{138}Ba ($\sim$1.32)] is 1.88$\sim$2.98, more than the critical value 1.825 in the Mallmann plot [78] showing undoubtedly the onset of collective characteristics. Moreover, these $R_{4/2}$ values lie between 1.82, the Mallmann critical point [78] and 3.0,

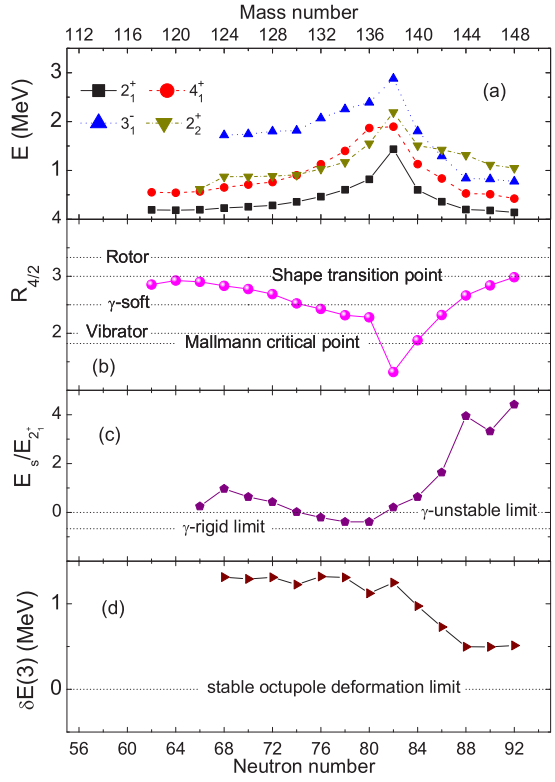

FIG. 4. (Color online) Energies of the first excited 2_1^+, 4_1^+, 3_1^- and the second 2_2^+ states (a), the ratio $R_{4/2}$ (b), the quantity E_S/E_{2^+} (c) and the energy difference $\delta E(3)$ (d) in even-even Ba isotopes as a function of the neutron (mass) number. See text for more details. The available experimental data are taken from Ref. [75].

the shape or phase transition point to quadrupole deformed nuclei [79,80], in good agreement with the facts of soft nuclei.

Deviations of the nuclear shape from axial symmetry can sensitively affect the second lowest 2_2^+ states (generally, the quasi-γ bandheads) of even-even nuclei. As shown in Fig. 4(a), the systematics of the relative location of such 2_2^+ states with respect to the ground-state band can be seen. Empirically, the quantity $E_S/E(2_1^+)$, $E_S = E(2_2^+) - E(4_1^+)$, can be as a global signature of the structural evolution involving axial asymmetry [81]. In the extreme γ-unstable limit [82], the value of $E_S/E(2_1^+)$ is zero due to the completely degenerate 2_2^+ and 4_1^+ states. In the case of a rigid-triaxial rotor with $25^\circ \leq \gamma \leq 30^\circ$ [83], the 2_2^+ state goes under the 4_1^+ level and reaches the bottom at the extreme of triaxiality with $\gamma = 30^\circ$ [$E_S/E(2_1^+) = -0.67$]. Therefore, nuclei with negative values of $E_S/E(2_1^+)$ between these two extremes 0 and -0.67 are most likely characterized by γ-soft potentials with shallow minima at the average γ value close to 30°. Meanwhile, the positive value of $E_s/E(2_1^+)$ indicates that the nucleus possesses an axially symmetric shape, because the 2_2^+ state lies at high excitation energy relative to the 2_1^+ and 4_1^+ states. The empirical $E_s/E(2_1^+)$ values for even-even $^{122-148}$Ba are presented in Fig. 4(c). One can see that three even-even nuclei $^{132-136}$Ba have negative $E_s/E(2_1^+)$ values (about -0.20, -0.38, and -0.38, respectively), less than the γ-rigid limit (-0.67). The smallest value (~ -0.38) in ^{134,136}Ba is still somewhat smaller than the empirical value of $E_S/E(2_1^+) \approx 0.5$, which is characteristic of the critical-point nuclei in terms of maximum γ softness between prolate and oblate shapes. This is in good agreement with our calculated result of $\gamma \sim 19^\circ$ in ^{134}Ba, as shown in Fig. 1(b), showing that the quantum phase transition from triaxial-prolate to triaxial-oblate shape in this nucleus occurs at low-lying rather than ground state. Nevertheless, the FY+FRDM calculation [40] indicates that such phase transition has already taken place at ground state in ^{134}Ba ($\beta_2 < 0$). It should be noted that a critical point of a prolate-oblate phase transition in γ-soft nuclei is discussed in the context of the O(6) limit of the interacting boson model, along with an interpretation in terms of Landau theory.

Stable octupole deformation or octupole softness in the body-fixed frame can be attributed to a parity-breaking odd-multipolarity interaction which couples intrinsic states of opposite parity. For normally deformed systems the condition for strong octupole coupling occurs for particle numbers near 34 ($g_{9/2} \otimes p_{3/2}$ coupling), 56 ($h_{11/2} \otimes d_{5/2}$ coupling), 88 ($i_{13/2} \otimes f_{7/2}$ coupling), and 134 ($j_{15/2} \otimes g_{9/2}$ coupling). In such nuclei, the level patterns are similar to rotational bands observed in reflection-asymmetric molecules including two bands of parity doublets characterized with simplex quantum numbers [61] $s = \pm 1$ or $s = \pm i$. The positive- and negative-parity rotational bands are intertwined by strong $E1$ transitions [69]. For even-even nuclei, the spins and parities of the levels in an octupole deformation band are $I^\pi = 0^+$, 1^-, 2^+, 3^-, ... for the $s = +1$ band, and $I^\pi = 0^-$, 1^+, 2^-, 3^+, ... for the $s = -1$ band. For odd-A nuclei, $I^\pi = 1/2^+$, $3/2^-$, $5/2^+$, $7/2^-$, ... for the $s = +i$ band, and $I^\pi = 1/2^-$, $3/2^+$, $5/2^-$, $7/2^+$, ... for the $s = -i$ band. In the Ba isotopic chain, the $s = +1$ bands have been observed in even-even ^{142,144,146}Ba [71,74] and the $s = \pm i$ bands of parity doublets have been observed in odd-A ^{143,145}Ba [72,73]. Some other Ba isotopes have no negative-parity band structures, even only one low-lying negative-parity state, decaying by relatively strong $E1$ transitions, is to date observed. This negative-parity state cannot easily be explained as a two-quasiparticle structure at the lowest spin and is usually proposed as possible evidence for octupole correlation. Figure 4(a) also shows the first low-lying 3_1^- states observed in the Ba isotopes. Obviously, such 3_1^- states have lower excited energies near neutron number 88. In addition, the energy differences δE between the $\pi = +$ and $\pi = -$ bands are used to evaluate the octupole deformation stability with spin variation, which can be deduced from the experimental level energies by using the relation [84]

$$\delta E(I) = E(I^-) - \frac{(I+1)E(I-1)^+ + (I)E(I+1)^+}{2I+1}. \quad (4)$$

Here the superscripts indicate the parities of the levels. In the limit of stable octupole deformation, $\delta E(I)$ should be close to zero. To discuss the octupole deformation instability at ground states, as seen in Fig. 4(d), we show the low-spin $\delta E(3)$ values obtained from the available data [75]. It is seen that the $\delta E(3)$ values are approximately large constant values from ^{124}Ba to ^{138}Ba, then decrease and approach the minimum at about $N = 88$, indicating that the octupole correlation in ^{144}Ba is stronger than that in other Ba nuclei.

Compared with Fig. 1, the evolutions of stiffness along different deformation directions can be qualitatively displayed by using the deformation energy curves (see Figs. 2–3) in theory and some phenomenological laws or ratios (see Fig. 4) in experiment. Based on a simple harmonic approximation, we have quantitatively investigated the stiffness evolution of 20 even-even Ba isotopes ranging from ^{112}Ba to ^{150}Ba in which both the collective (quadrupole and/or octupole) excited states and the quasiparticle excited states are observed or to be observed in experiments. The stiffness constants C_2, C_γ, and C_3 are determined numerically from the deformation energy curves with respect to β_2, γ, and β_3. For instance, the stiffness parameter C_2 is defined from the equation [3]

$$E = E_{\min} + \tfrac{1}{2}C_2\left(\beta_2 - \beta_2^{\min}\right)^2, \tag{5}$$

where the constant C_2 is extracted from the minimum energy $E_{\min}$ at $\beta_2 = \beta_2^{\min}$ and $\beta_2 = \beta_2^{\min} \pm \Delta\beta_2$. We use a step size $\Delta\beta_2 \cong 0.05$ in this mass region. Such a step size yields results in the harmonic approximation that are close to those calculated with the WKB approximation, in which anharmonicities in the potential energy are taken into account [48]. Similarly, we evaluate the stiffness constants C_γ and C_3 from

$$E = E_0 + \tfrac{1}{2}C_\kappa\kappa^2, \tag{6}$$

with $\kappa = \gamma$ or β_3 denoting the deformation degrees of freedom in the γ and β_3 directions, respectively. The corresponding step sizes $\Delta\gamma \cong 10^\circ$ and $\Delta\beta_3 \cong 0.05$ are adopted in the calculations. (Note that slightly different step sizes give similar results.) The calculated stiffness coefficients in the β_2, γ, and β_3 directions are shown in Fig. 5. One sees that the general trend of the C_2 coefficients calculated in the different deformation spaces is consistent, though they are somewhat different. The smallest β_2 stiffness (largest softness) occurs in the $N = 82$ (shell closure) nucleus ^{138}Ba. Similar to the discussions in Ref. [21], the stiffness constant $C_\gamma > 0$ ($C_3 > 0$) corresponds to the γ (octupole) vibrational limit; the system becomes unstable to γ (octupole) vibrations at $C_\gamma = 0$ ($C_3 = 0$) and is permanently deformed for $C_\gamma < 0$ ($C_3 < 0$). As shown in Fig. 5, the stiffness constant C_γ exhibits an irregular oscillating behavior. The strong γ correlations expectedly occur at around $N = 64$ and 76. Simultaneously, one can see from Fig. 5 that the octupole stiffness coefficients C_3 keep constant from ^{116}Ba to ^{136}Ba and decrease as N approaches 56 or 88, in good agreement with the analysis of the available $\delta E(3)$ data (see Fig. 4). Figure 5 also shows that there is hardly overlap between strong γ ($C_\gamma \leqslant 0$) and octupole ($C_3 \leqslant 0$) correlation regions. However, it is noticed that both C_γ and C_3 decrease as N approaches 56, indicating simultaneously increasing γ and octupole correlations. This is consistent with previous study by Skalski [85], where the coupling between γ and β_3 deformations is discussed and a possible transition to the triaxial-octupole shape in ^{112}Ba is suggested.

To crudely test the validity of the WS potential (mean-field) parameters and the LN pairing method, we have investigated the Fermi energy levels, with the energy of the last occupied single-particle level, and the LN pairing gap, respectively. Comparisons have been made with the related quantities

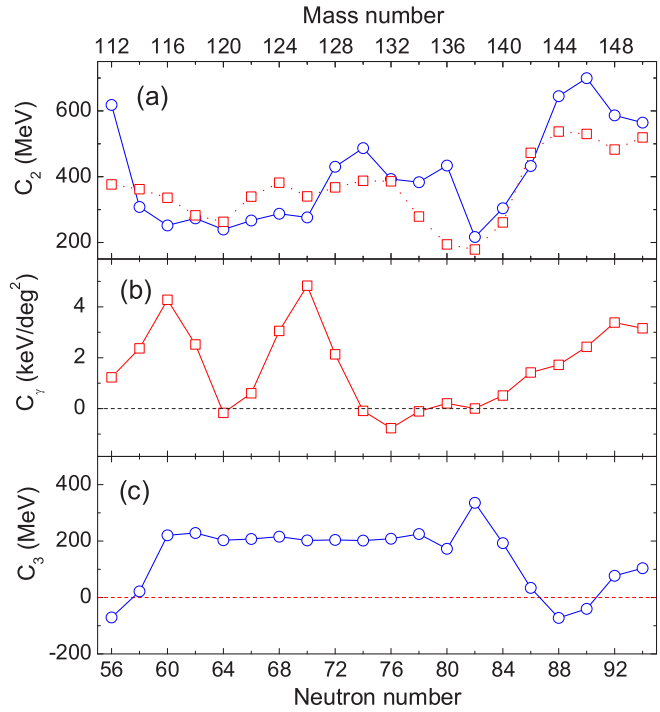

FIG. 5. (Color online) Calculated stiffness coefficients C_2 (a), C_γ (b), and C_3 (c) towards β_2, γ, and β_3 deformations for even-even $^{112-150}$Ba nuclei. The square and circle symbols indicate that the calculations are performed in (β_2,γ,β_4) and (β_2, β_3, β_4, β_5) deformation spaces, respectively.

in experiments and/or other theories, as seen in Figs. 6 and 7. Figure 6 shows the trend of the calculated proton and neutron Fermi energy levels determined by the universal potential parameters is expectedly consistent with that of the two-proton and two-neutron separation energies and that of the lifetime data. It is worth noting that the proton Fermi energy levels has positive energies for $N \leqslant 58$, indicating such protons are quasibound or unbound (the Coulomb barrier may inhibit proton emission). The standard way of extracting the shell correction may break down for such weakly bound nuclei where the contribution from the particle continuum becomes important [86]. In this investigation, the positive-energy spectrum was approximated by quasibound states. That is, even the pairing window includes positive energy states, particles do not scatter into the continuum by the pairing force. The single-particle picture, which only serves as the set of basis functions for the shell and pairing calculations, does not give the true nuclear ground or excited states. Such procedure should not be considered as satisfactory. A proper treatment of continuum states is usually achieved with either the Wigner-Kirkwood expansion or Green's function methods [86,87]. It should be pointed out that an additional p-n channel for the nuclear force, namely, the $T = 0$ component, appears in $Z \sim N$ nuclei since the Pauli principle is not active between protons and neutrons, indicating a possibly increasing binding force of nucleons. It is estimated that five additional nuclei beyond the proton drip line could live long enough to be observed in this Ba isotopic chain [88]. Near

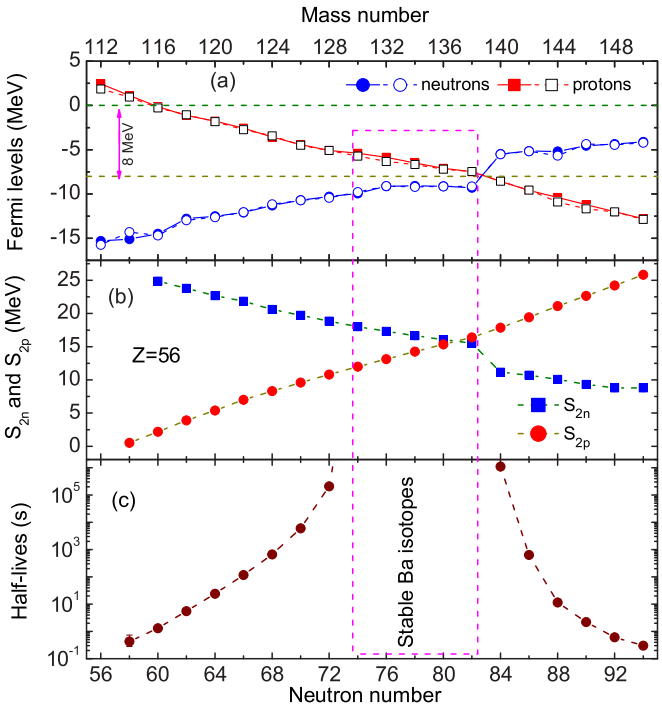

FIG. 6. (Color online) (a) Calculated neutron and proton Fermi energy levels for even-even $^{112-150}$Ba nuclei with the calculated equilibrium shapes as input quantities [90]. Note that the filled and open symbols indicate that the calculations are performed in $(\beta_2, \gamma, \beta_4)$ and $(\beta_2, \beta_3, \beta_4, \beta_5)$ deformation spaces, respectively. (b) Available two-proton and two-neutron separation energies for the Ba isotopic chain. (c) Available half-lives of known Ba isotopes [75], indicating the nuclear instabilities. Note that the half-life for ^{132}Ba is greater than 10^{28} s.

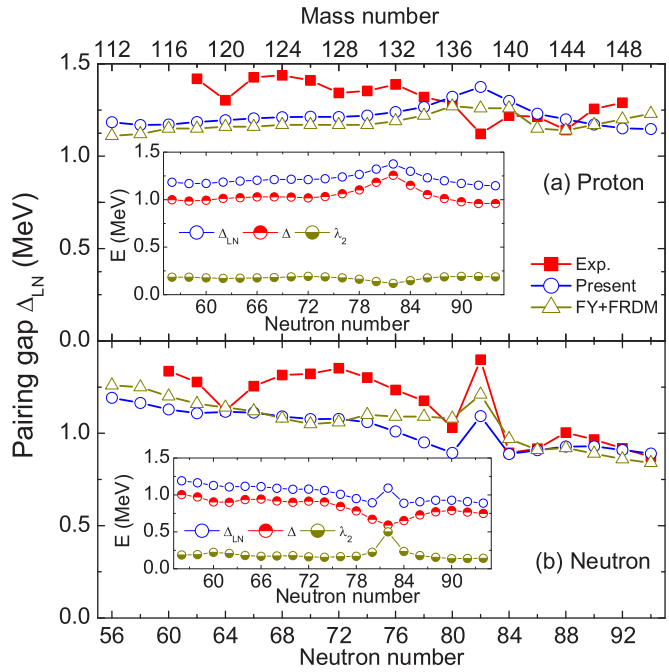

FIG. 7. (Color online) Calculated LN pairing gaps of proton and neutron for even-even $^{112-150}$Ba nuclei, compared with the FY+FRDM calculations [90] and experiments. The insets indicate the contributions of the pairing gap Δ and the number-fluctuation constant λ_2 to the LN pairing gap Δ_{LN}. See text for more details.

^{112}Ba, previous studies [21,89] have pointed out that there are the coherent contributions of $\pi(\nu)d_{5/2}$-$\nu(\pi)h_{11/2}$ coupling terms to octupole correlations from both valence neutrons and protons which almost occupy identical orbitals of the $2d_{5/2}$ and $1h_{11/2}$ subshells, as well as the increasing n-p pairing gap and n-p quadrupole-quadrupole coupling strength due to the increasing n-p symmetry.

Figure 7 shows the pairing gaps of proton and neutron calculated by using the LN pairing model for even-even $^{112-150}$Ba nuclei, compared with the FY+FRDM calculations [90] and the experimental values extracted from experimental masses [91] by use of fourth-order finite-difference expressions [92]. In the present method, a pairing gap Δ and number-fluctuation constant λ_2 are obtained as solutions of the pairing equations. The Δ_{LN} values representing the sum $\Delta + \lambda_2$ can be crudely compared with the experimental odd-even mass differences. Generally speaking, the calculated Δ_{LN} trend is consistent with the FY+FRDM calculations, somewhat smaller than the experimental values, as shown in Fig. 7. There is no collapse at magic neutron numbers, in contrast to results based on the BCS approximation. One can see from the insets of Fig. 7 that the proton pairing gap Δ on the whole increases as the neutron magic number $N = 82$ is approached. This increase is partly canceled out by a decrease in λ_2, which results in a relatively smooth appearance of Δ_{LN} at the magic neutron number. In contrast, the individual neutron contribution Δ decreases considerably near the neutron magic number $N = 82$ and such a decrease is compensated for by a strong increase in neutron λ_2, so that their sum behaves relatively smoothly and especially reproduces the experimental property of a sudden increase at $N = 82$, as seen in Fig. 7(b). To more appropriately compare with the experimental value, as discussed in Ref. [90], the pairing gap is suggested to determine directly from odd-even mass differences based on theoretical masses, where the nonsmooth contributions given by spherical (even deformed) gaps and shape transitions may cancel out to some extent. However, it turns out that, even so, the corresponding theoretical mass differences are still systematically smaller than the experimental ones [92] (in principle, they should be identical). Some effects such as mean-field and odd-nucleon effects are pointed out to be responsible for this discrepancy [93,94]. Actually, when such effects are taken into account, pairing strengths are increased by about 5–10% (at least in the rare-earth region), resulting in larger pairing gaps [92]. In the present work focusing on stiffness evolutions, we have not performed the pairing strength adjustment since such an operation affects the ground-state deformation very slightly [45].

In addition, as is known, the realistic phenomenological WS potential provides a good description of not only the ground-state properties but also the excited-state properties of nuclei. For instance, such a phenomenological potential has been successfully applied to explain and predict the nuclear equilibrium deformations, the high-K isomer, the nucleon binding energies, the fission barriers, and a number of the

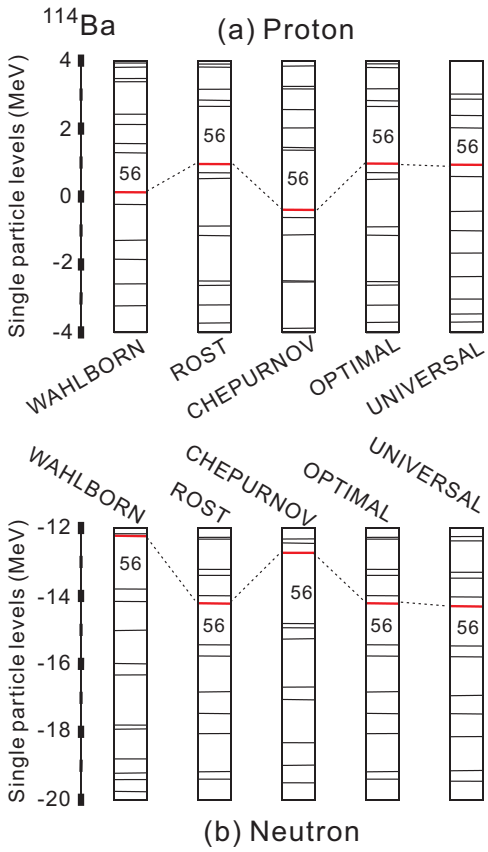

FIG. 8. (Color online) Calculated proton (a) and neutron (b) single-particle levels near their Fermi surfaces for neutron-deficient ^{114}Ba based on different set of WS parameters [58]. The red levels connected by dotted lines denote the Fermi levels.

single-particle effects for superdeformed and fast rotating nuclei, etc. (see [32,46,47,58,92] and references therein). Various parametrizations of the WS potential have been fitted to the contemporarily existing experimental data with a different emphasis on nuclear structure properties. Most of the existing WS parameter sets are only suitable for a certain nuclear mass region. Even, for the so-called universal parameters, which are N and Z independent, special attention should be paid when extrapolating to the drip-line region. Just to see the parameter dependence in the very neutron-deficient ^{114}Ba, five frequently used WS parametrizations—Blomqvist and Wahlborn [55], Chepurnov [56], and Rost [57], optimal [58], and universal [58]—have been implemented to calculate the single-particle level near the Fermi surface, as shown in Fig. 8. One can see that the single-particle states located around the Fermi level are considerably affected by the WS parameter sets, implying a possibly large effect on the shell and pairing corrections.

Recently, the isospin dependences of the spin-orbit potential and the nuclear surface diffuseness have been revealed to be important factors in the accurate description of the ground-state properties of nuclei, in particular near the drip lines [95,96]. Moreover, the angular dependence of surface diffuseness is further discussed by Adamian *et al.* [97]. It is of

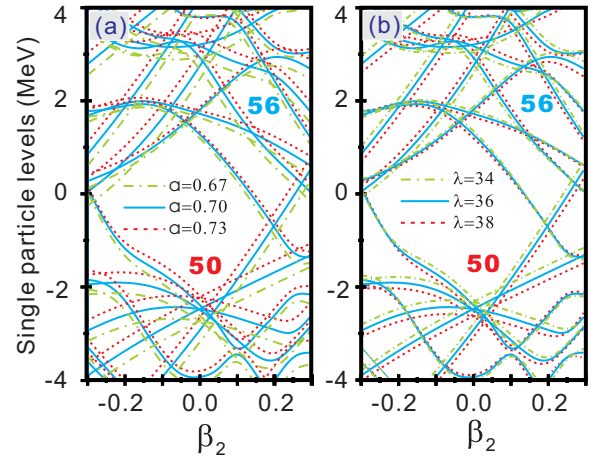

FIG. 9. (Color online) Calculated proton single-particle levels for ^{114}Ba as functions of quadrupole deformation β_2. Part (a) shows results for three selected surface diffuseness a values (0.67, 0.70, and 0.73 fm) and all other potential parameters are identical with those of universal values [58]. Part (b) is similar to (a) but for different spin-orbit strengths λ (34.0, 36.0, and 38.0).

interest to examine whether and to what extent the present results will be changed if the model parameters (e.g., the strength of the spin-orbit potential λ, and the nuclear surface diffuseness a) are adjusted. As an example, the near-drip-line ^{114}Ba nucleus is investigated here. As shown in Fig. 9, the single-proton levels are given to display the effects of the spin-orbit coupling strength and the nuclear surface diffuseness. According to Ref. [95], the parameters (a, λ) are slightly modified on the basis of the initial values (0.70, 36), namely, the universal values. Certainly, it is hoped that $a = 0.73$ and $\lambda = 38$ should be more suitable for the present case based on the function relationship of the isospin dependence of such two parameters in Ref. [95]. It can be noticed from Fig. 9(a) that the increase of the diffuseness parameter a mainly pushes up the single-particle spectrum while the relative distances between them vary rather slightly. Figure 9(b) shows that some levels are pulled down and, simultaneously, other ones are pushed up with the increasing spin-orbit coupling strength λ. This means, as expected, that λ can control the relative positions of levels.

Figure 10 shows the deformation energy curves for the selected ^{114}Ba nucleus calculated by using the modified (λ, a) parameters. It is found that the ground-state equilibrium deformation is stable against various (λ, a) combinations. The stiffness related to the curvature at the minimum of the energy curve is affected slightly. However, the depth of the minimum is changed to some extent, which results in the variation of the binding energy (mass), agreeing with the discussion in Ref. [95]. In addition, as shown in Fig. 10, such slight parameter modifications may have important influence on the barrier (the energy difference between the minimum and the saddle point at PES). Nowadays, it is known that the axial (reflection) asymmetry in the nuclear shape affects the inner (outer) fission barrier for the heavier actinides and superheavy nuclei [98–101]. According to present investigation, we have no reason to doubt that the adjustment of λ and/or a can affect

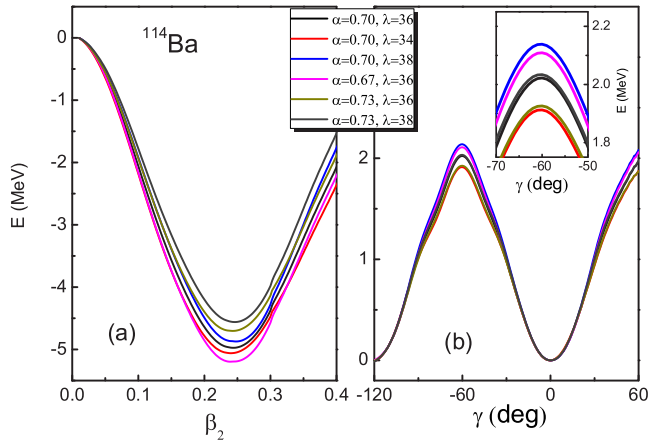

FIG. 10. (Color online) Similar to Fig. 2 but for different parameter combinations of the surface diffuseness a and spin-orbit strength λ for the selected ^{114}Ba nucleus. All other potential parameters are identical with those of universal values [58].

the fission barrier for such nuclei, though it is beyond the scope of this work.

IV. SUMMARY

In summary, we have calculated the ground-state equilibrium deformations for even-even $^{112-150}$Ba isotopes based on the pairing-deformation self-consistent PES methods in the multidimensional (β_2,γ,β_4) and $(\beta_2, \beta_3, \beta_4, \beta_5)$ deformation spaces, where the phenomenological nuclear mean-field model with the WS Hamiltonian using the universal parameters is employed. The calculated values are to a great extent in good agreement with previous theoretical results and available experimental data. The β_2, γ, and β_3 deformation energy curves are analyzed in detail, which is helpful to understand the structural evolution of these nuclei. In particular, the variation of β_2, γ, and β_3 stiffness with neutron number are discussed. The present results reveal that the γ-soft or triaxial (octupole-soft or octupole-deformed) nuclei have relatively large stiffness in the direction of octupole (γ) degrees of freedom, at least, for the ground states. It seems, obviously, that in such phenomenological nuclear mean-field calculations, to ensure the right nuclear shape without unnecessary losses of CPU time the selection of the deformation space (namely, what deformation degrees of freedom need to be considered) should be of importance. Of course, as known, there is no doubt that the Coriolis effect can induce an onset of reflection and axial asymmetries of a nuclear system to a large extent. Very recently, for instance, Mazurek *et al.* discussed the competition between the so-called nuclear Jacobi (from axially symmetric to the triaxially symmetric configurations) and Poincaré (from reflection-symmetric to the reflection-asymmetric configurations) shape transitions at high spins and temperatures [33]. Moreover, such shape transitions have been predicted and discussed in a few barium nuclei [102,103]. Therefore, the more reasonable PES calculation concerning rotation should simultaneously consider nonaxiality, reflection asymmetry, and the isospin dependence of the spin-orbit potential and the nuclear surface diffuseness, and even the angular dependence of surface diffuseness.

The observation of low-lying negative-parity states in $^{114-116}$Ba (only the ground states of these nuclei have been hitherto identified [75]) would also be of great interest, which would present a valuable insight into octupole collectivity in this region. Though in-beam spectroscopy of barium isotopes with $A < 118$ with stable beams and targets will prove to be very difficult since the proximity to the drip lines strongly depends on new experimental devices, in particular radioactive ion beam accelerators and γ-ray tracking arrays, these nuclei are still excellent candidates to be studied once suitable radioactive-ion beams have been developed.

ACKNOWLEDGMENTS

One of the authors (H.L.W.) would like to thank the referee and Professor Jerzy Dudek for helpful suggestions on the manuscript. This work is supported by the Natural Science Foundation of China (Grants No. 10805040 and No. 11175217), the Foundation and Advanced Technology Research Program of Henan Province (Grant No. 132300410125) and the S&T Research Key Program of Henan Province Education Department (Grant No. 13A140667).

[1] S. Frauendorf, Rev. Mod. Phys. **73**, 463 (2001).
[2] N. J. Stone, At. Data Nucl. Data Tables **90**, 75 (2005).
[3] W. Nazarewicz, P. Olanders, I. Ragnarsson, J. Dudek, G. A. Leander, P. Möller, and E. Ruchowsa, Nucl. Phys. A **429**, 269 (1984).
[4] R. F. Casten and E. A. McCutchan, J. Phys. G: Nucl. Part. Phys. **34**, R285 (2007).
[5] R. F. Casten, Prog. Part. Nucl. Phys. **62**, 183 (2009).
[6] P. Cejnar, J. Jolie, and R. F. Casten, Rev. Mod. Phys. **82**, 2155 (2010).
[7] W. Nazarewicz, Prog. Part. Nucl. Phys. **28**, 307 (1992).
[8] W. J. Świątecki, Phys. Rev. **104**, 993 (1956).
[9] S. Cohen and W. Świątecki, Ann. Phys. (NY) **22**, 406 (1963).
[10] W. Greiner and J. A. Maruhn, *Nuclear Models* (Springer-Verlag, Berlin, Heidelberg, 1996).
[11] A. Bohr and B. R. Mottelson, *Nuclear Structure*, Vol. II (World Scientific, Singapore, 1998).
[12] P. Ring and P. Schuck, *The Nuclear Many-body Problem* (Springer-Verlag, Berlin, 1980).
[13] S. G. Nilsson, C. F. Tsang, A. Sobiczewski, Z. Szymanski, S. Wycech, C. Gustafson, I.-L. Lamm, P. Möller, and B. Nilsson, Nucl. Phys. A **131**, 1 (1969).
[14] S. Trentalange, S. E. Koonin, and A. J. Sierk, Phys. Rev. C **22**, 1159 (1980).
[15] P. Stránský, A. Frank, and R. Bijker, J. Phys.: Conf. Ser. **322**, 012018 (2011).

[16] S. W. Ødegård, G. B. Hagemann, D. R. Jensen, M. Bergström, B. Herskind, G. Sletten, S. Törmänen, J. N. Wilson, P. O. Tjøm, I. Hamamoto, K. Spohr, H. Hübel, A. Görgen, G. Schönwasser, A. Bracco, S. Leoni, A. Maj, C. M. Petrache, P. Bednarczyk, and D. Curien, Phys. Rev. Lett. **86**, 5866 (2001).

[17] R. Bengtsson, H. Frisk, F. R. May, and J. A. Pinston, Nucl. Phys. A **415**, 189 (1984).

[18] K. Starosta, T. Koike, C. J. Chiara, D. B. Fossan, D. R. LaFosse, A. A. Hecht, C. W. Beausang, M. A. Caprio, J. R. Cooper, R. Krücken, J. R. Novak, N. V. Zamfir, K. E. Zyromski, D. J. Hartley, D. L. Balabanski, Jing-ye Zhang, S. Frauendorf, and V. I. Dimitrov, Phys. Rev. Lett. **86**, 971 (2001).

[19] S. Frauendorf and J. Meng, Nucl. Phys. A **617**, 131 (1997).

[20] J. Meng and S. Q. Zhang, J. Phys. G: Nucl. Part. Phys. **37**, 064025 (2010).

[21] P. A. Butler and W. Nazarewicz, Rev. Mod. Phys. **68**, 349 (1996).

[22] X. Li and J. Dudek, Phys. Rev. C **49**, R1250 (1994).

[23] S. Takami, K. Yabana, and M. Matsuo, Phys. Lett. B **431**, 242 (1998).

[24] M. Yamagami and K. Matsuyanagi, Nucl. Phys. A **672**, 123 (2000).

[25] M. Yamagami, K. Matsuyanagi, and M. Matsuo, Nucl. Phys. A **693**, 579 (2001).

[26] J. Dudek, A. Góźdź, N. Schunck, and M. Miśkiewicz, Phys. Rev. Lett. **88**, 252502 (2002).

[27] J. Dudek, D. Curien, N. Dubray, J. Dobaczewski, V. Pangon, P. Olbratowski, and N. Schunck, Phys. Rev. Lett. **97**, 072501 (2006).

[28] Y.-S. Chen, Y. Sun, and Z.-C. Gao, Phys. Rev. C **77**, 061305(R) (2008).

[29] A. P. Robinson, T. L. Khoo, I. Ahmad, S. K. Tandel, F. G. Kondev, T. Nakatsukasa, D. Seweryniak, M. Asai, B. B. Back, M. P. Carpenter, P. Chowdhury, C. N. Davids, S. Eeckhaudt, J. P. Greene, P. T. Greenlees, S. Gros, A. Heinz, R.-D. Herzberg, R. V. F. Janssens, G. D. Jones, T. Lauritsen, C. J. Lister, D. Peterson, J. Qian, U. S. Tandel, X. Wang, and S. Zhu, Phys. Rev. C **78**, 034308 (2008).

[30] J. Zhao, B.-N. Lu, E.-G. Zhao, and S.-G. Zhou, Phys. Rev. C **86**, 057304 (2012).

[31] J. Dudek, D. Curien, A. Góźdź, Y. R. Shimizu, and S. Tagami, Acta Phys. Pol. B **44**, 305 (2013).

[32] H. L. Liu, F. R. Xu, P. M. Walker, and C. A. Bertulani, Phys. Rev. C **83**, 011303(R) (2011).

[33] K. Mazurek, J. Dudek, A. Maj, and D. Rouvel, Phys. Rev. C **91**, 034301 (2015).

[34] I. Tanihata, H. Hamagaki, O. Hashimoto, Y. Shida, N. Yoshikawa, K. Sugimoto, O. Yamakawa, T. Kobayashi, and N. Takahashi, Phys. Rev. Lett. **55**, 2676 (1985).

[35] I. Tanihata, D. Hirata, T. Kobayashi, S. Shimoura, K. Sugimoto, and H. Toki, Phys. Lett. B **289**, 261 (1992).

[36] T. Suzuki, H. Geissel, O. Bochkarev, L. Chulkov, M. Golovkov, D. Hirata, H. Irnich, Z. Janas, H. Keller, T. Kobayashi, G. Kraus, G. Münzenberg, S. Neumaier, F. Nickel, A. Ozawa, A. Piechaczeck, E. Roeckl, W. Schwab, K. Sümmerer, K. Yoshida, and I. Tanihata, Phys. Rev. Lett. **75**, 3241 (1995).

[37] A. Shore, A. Fritsch, J. Q. Ginepro, M. Heim, A. Schuh, and M. Thoennessen, At. Data Nucl. Data Tables **96**, 749 (2010).

[38] R. C. Nayak and L. Satpathy, At. Data Nucl. Data Tables **98**, 616 (2012).

[39] P. Möller and J. R. Nix, At. Data Nucl. Data Tables **59**, 185 (1995).

[40] P. Möller, R. Bengtsson, B. G. Carlsson, P. Olivius, T. Ichikawa, H. Sagawa, and A. Iwamoto, At. Data Nucl. Data Tables **94**, 758 (2008).

[41] Y. Aboussir, J. M. Pearson, A. K. Dutta, and Tondeur, At. Data Nucl. Data Tables **61**, 127 (1995).

[42] H.-L. Wang, H.-L. Liu, F.-R. Xu, and C.-F. Jiao, Prog. Theor. Phys. **128**, 363 (2012).

[43] H.-L. Wang, H.-L. Liu, and F.-R. Xu, Phys. Scr. **86**, 035201 (2012).

[44] Q.-Z. Chai, H.-L. Wang, Q. Yang, and M.-L. Liu, Chin. Phys. C **39**, 024101 (2015).

[45] F. R. Xu, P. M. Walker, J. A. Sheikh, and R. Wyss, Phys. Lett. B **435**, 257 (1998).

[46] H. L. Liu, F. R. Xu, S. W. Xu, R. Wyss, and P. M. Walker, Phys. Rev. C **76**, 034313 (2007).

[47] Y. Shi, P. M. Walker, and F. R. Xu, Phys. Rev. C **85**, 027307 (2012).

[48] P. Möller and J. R. Nix, Nucl. Phys. A **361**, 117 (1981).

[49] W. D. Myers and W. J. Swiatecki, Nucl. Phys. A **81**, 1 (1966).

[50] W. Satuła, R. Wyss, and P. Magierski, Nucl. Phys. A **578**, 45 (1994).

[51] W. Nazarewicz, M. A. Riley, and J. D. Garrett, Nucl. Phys. A **512**, 61 (1990).

[52] H. C. Pradhan, Y. Nogami, and J. Law, Nucl. Phys. A **201**, 357 (1973).

[53] V. M. Strutinsky, Nucl. Phys. A **95**, 420 (1967).

[54] W. Satuła and R. Wyss, Rep. Prog. Phys. **68**, 131 (2005).

[55] J. Blomqvist and S. Wahlborn, Ark. Fys. **16**, 543 (1960).

[56] V. A. Chepurnov, Yad. Fiz. **6**, 955 (1967).

[57] E. Rost, Phys. Lett. B **26**, 184 (1968).

[58] S. Ćwiok, J. Dudek, W. Nazarewicz, J. Skalski, and T. Werner, Comp. Phys. Comm. **46**, 379 (1987).

[59] W. Satuła and R. Wyss, Phys. Rev. C **50**, 2888 (1994).

[60] P. Möller and J. R. Nix, Nucl. Phys. A **536**, 20 (1992).

[61] W. Nazarewicz, G. A. Leander, and J. Dudek, Nucl. Phys. A **467**, 437 (1987).

[62] S. Raman, C. W. Nestor, Jr., and P. Tikkanen, At. Data Nucl. Data Tables **78**, 1 (2001).

[63] L. Grodzins, Phys. Lett. **2**, 88 (1962).

[64] F. S. Stephens, R. M. Diamond, J. R. Leigh, T. Kammuri, and K. Nakai, Phys. Rev. Lett. **29**, 438 (1972).

[65] J. Dudek, W. Nazarewicz, and P. Olanders, Nucl. Phys. A **420**, 285 (1984).

[66] M. O. Kortelahti, B. D. Kern, R. A. Braga, R. W. Fink, I. C. Girit, and R. L. Mlekodaj, Phys. Rev. C **42**, 1267 (1990).

[67] B. D. Kern, R. L. Mlekodaj, G. A. Leander, M. O. Kortelahti, E. F. Zganjar, R. A. Braga, R. W. Fink, C. P. Perez, W. Nazarewicz, and P. B. Semmes, Phys. Rev. C **36**, 1514 (1987).

[68] W. Nazarewicz, J. Dudek, R. Bengtsson, T. Bengtsson, and I. Ragnarsson, Nucl. Phys. A **435**, 397 (1985).

[69] W. Nazarewicz, P. Olanders, I. Ragnarsson, J. Dudek, and G. A. Leander, Phys. Rev. Lett. **52**, 1272 (1984).

[70] J. H. Hamilton, A. V. Ramayya, S. J. Zhu, G. M. Ter-Akopian, Yu. Ts. Oganessian, J. D. Cole, J. O. Rasmussen, and M. A. Stoyer, Prog. Part. Nucl. Phys. **35**, 635 (1995).

[71] S. J. Zhu, Q. H. Lu, J. H. Hamilton, A. V. Ramayya, L. K. Peker, M. G. Wang, W. C. Ma, B. R. S. Babu, T. N. Ginter, J. Kormicki, D. Shi, J. K. Deng, W. Nazarewicz, J. O. Rasmussen, M. A. Stoyer, S. Y. Chu, K. E. Gregorich, M. F. Mohar, S. Asztalos,

S. G. Prussin, J. D. Cole, R. Aryaeinejad, Y. K. Dardenne, M. Drigert, K. J. Moody, R. W. Loughed, J. F. Wild, N. R. Johnson, I. Y. Lee, F. K. McGowan, G. M. Ter-Akopian, and Yu. Ts. Oganessian, Phys. Lett. B **357**, 273 (1995).
[72] M. A. Jones, W. Urban, J. L. Durell, M. Leddy, W. R. Phillips, A. G. Smith, B. J. Varley, I. Ahmad, L. R. Morss, M. Bentaleb, E. Lubkiewicz, and N. Schulz, Nucl. Phys. A **605**, 133 (1996).
[73] S. J. Zhu, J. H. Hamilton, A. V. Ramayya, E. F. Jones, J. K. Hwang, M. G. Wang, X. Q. Zhang, P. M. Gore, L. K. Peker, G. Drafta, B. R. S. Babu, W. C. Ma, G. L. Long, L. Y. Zhu, C. Y. Gan, L. M. Yang, M. Sakhaee, M. Li, J. K. Deng, T. N. Ginter, C. J. Beyer, J. Kormicki, J. D. Cole, R. Aryaeinejad, M. W. Drigert, J. O. Rasmussen, S. Asztalos, I. Y. Lee, A. O. Macchiavelli, S. Y. Chu, K. E. Gregorich, M. F. Mohar, G. M. Ter-Akopian, A. V. Daniel, Yu. Ts. Oganessian, R. Donangelo, M. A. Stoyer, R. W. Lougheed, K. J. Moody, J. F. Wild, S. G. Prussin, J. Kliman, and H. C. Griffin, Phys. Rev. C **60**, 051304(R) (1999).
[74] W. R. Phillips, I. Ahmad, H. Emling, R. Holzmann, R. V. F. Janssens, T. L. Khoo, and M. W. Drigert, Phys. Rev. Lett. **57**, 3257 (1986).
[75] http://www.nndc.bnl.gov/chart/
[76] W. Andrejtscheff and P. Petkov, Phys. Rev. C **48**, 2531 (1993).
[77] W. Andrejtscheff and P. Petkov, Phys. Lett. B **329**, 1 (1994).
[78] M. A. J. Mariscotti, Phys. Rev. Lett. **24**, 1242 (1970).
[79] F. Iachello, N. V. Zamfir, and R. F. Casten, Phys. Rev. Lett. **81**, 1191 (1998).
[80] R. F. Casten, D. Kusnezov, and N. V. Zamfir, Phys. Rev. Lett. **82**, 5000 (1999).
[81] H. Watanabe, K. Yamaguchi, A. Odahara, T. Sumikama, S. Nishimura, K. Yoshinaga, Z. Li, Y. Miyashita, K. Sato, L. Próchniak, H. Baba, J. S. Berryman, N. Blasi, A. Bracco, F. Camera, J. Chiba, P. Doornenbal, S. Go, T. Hashimoto, S. Hayakawa, C. Hinke, N. Hinohara, E. Ideguchi, T. Isobe, Y. Ito, D. G. Jenkins, Y. Kawada, N. Kobayashi, Y. Kondo, R. Krücken, S. Kubono, G. Lorusso, T. Nakano, T. Nakatsukasa, M. Kurata-Nishimura, H. J. Ong, S. Ota, Zs. Podolyák, H. Sakurai, H. Scheit, K. Steiger, D. Steppenbeck, K. Sugimoto, K. Tajiri, S. Takano, A. Takashima, T. Teranishi, Y. Wakabayashi, P. M. Walker, O. Wieland, and H. Yamaguchi, Phys. Lett. B **704**, 270 (2011).
[82] L. Wilets and M. Jean, Phys. Rev. **102**, 788 (1956).
[83] A. S. Davydov and G. F. Filippov, Nucl. Phys. **8**, 237 (1958).
[84] W. Nazarewicz and P. Olanders, Nucl. Phys. A **441**, 420 (1985).
[85] J. Skalski, Phys. Rev. C **43**, 140 (1991).
[86] W. Nazarewicz, T. R. Werner, and J. Dobaczewski, Phys. Rev. C **50**, 2860 (1994).
[87] T. Vertse, A. T. Kruppa, and W. Nazarewicz, Phys. Rev. C **61**, 064317 (2000).
[88] M. Thoennessen, Rep. Prog. Phys. **67**, 1187 (2004).
[89] D. S. Delion, R. Wyss, R. J. Liotta, Bo Cederwall, A. Johnson, and M. Sandzelius, Phys. Rev. C **82**, 024307 (2010).
[90] P. Möller, J. R. Nix, and K.-L. Kratz, At. Data Nucl. Data Tables **66**, 131 (1997).
[91] M. Wang, G. Audi, A. H. Wapstra, F. G. Kondev, M. MacCormick, X. Xu, and B. Pfeiffer, Chin. Phys. C **36**, 1603 (2012).
[92] F. R. Xu, R. Wyss, and P. M. Walker, Phys. Rev. C **60**, 051301 (1999).
[93] J. Y. Zeng and T. S. Cheng, Nucl. Phys. **405**, 1 (1983).
[94] W. Satuła, J. Dobaczewski, and W. Nazarewicz, Phys. Rev. Lett. **81**, 3599 (1998).
[95] N. Wang, M. Liu, X. Z. Wu, and J. Meng, Phys. Lett. B **734**, 215 (2014).
[96] Q. Zhi and Z. Ren, Phys. Lett. B **638**, 166 (2006).
[97] G. G. Adamian, N. V. Antonenko, L. A. Malov, G. Scamps, and D. Lacroix, Phys. Rev. C **90**, 034322 (2014).
[98] V. V. Pashkevich, Nucl. Phys. A **133**, 400 (1969).
[99] P. Möller and S. G. Nilsson, Phys. Lett. B **31**, 283 (1970).
[100] H. Schultheis, R. Schultheis, and G. Sussmann, Nucl. Phys. A **144**, 545 (1970).
[101] B.-N. Lu, E.-G. Zhao, and S.-G. Zhou, Phys. Rev. C **85**, 011301(R) (2012).
[102] A. Maj, K. Mazurek, J. Dudek, M. Kmiecik, and D. Rouvel, Int. J. Mod. Phys. E **19**, 532 (2010).
[103] K. Mazurek, J. Dudek, M. Kmiecik, A. Maj, J. P. Wieleczko, and D. Rouvel, Acta Phys. Pol. B **42**, 471 (2011).